Preparation and Study of Polyacryamide-Stabilized Silver Nanoparticles through a One-Pot Process

Meng Chen,*,†,‡ Li-Ying Wang,† Jian-Tao Han,† Jun-Yan Zhang,‡ Zhi-Yuan Li,§ and Dong-Jin Qian*,†

Department of Chemistry and Laboratory of Advanced Materials, Fudan University, 220 Handan Road, Shanghai 200433, P R China, State Key Laboratory of Solid Lubrication, Lanzhou Institute of Chemical Physics, Chinese Academy of Science, Lanzhou 730000, P R China, and Institute of Physics, Chinese Academy of Science, Beijing 100080, P R China

Received: February 22, 2006; In Final Form: April 18, 2006

A one-pot route was illustrated to synthesize stable well-dispersed silver colloids stabilized by polyacrylamide on a large scale. Reduction of silver ions and polymerization of acrylamide occurred almost simultaneously in the absence of a commonly used reducing agent and initiator. A possible mechanism for the formation of silver nanoparticles with bimodal size distribution was proposed. The structure and composition of the obtained nanoparticles were characterized carefully. Furthermore, light scattering simulation and UV−vis absorption studies confirmed that the obtained colloids were the mixture of Ag and Ag_2O nanoparticles. The presence of silver oxide layers on the nanoparticle surface should be responsible for the broadening of the surface plasmon band of silver nanoparticles. Ag_2O layers could be added or removed from Ag nanoparticle surfaces by the addition of HNO_3, HAc, or NaCl solution to the as-obtained silver colloids.

I. Introduction

The unique size- and shape-dependent optical,[1−4] catalysis,[5] and antimicrobial[6,7] properties of silver nanoparticles have prompted increasing interest of chemists, physicists, and materials scientists. Especially silver materials with zero-, one-, or two-dimensional nanostructures such as monodisperse nanoparticles,[8−11] nanowires,[12−16] nanodisks,[17−19] nanoprisms,[20,21] nanoplates,[22,23] and nanocubes[24,25] are believed to have great potential for applications in optics, catalysis, and other fields.

A number of reports are available in the literature for the solution synthesis of silver nanoparticles. Reduction routes involved in these studies fall into three broadly defined categories. The first one involves the use of relatively strong reducing agents, such as sodium borohydride,[26−32] hydrazine,[9,10] and tetrabutylammonium borohydride,[9] to prepare silver nanoparticles. The second one is the irradiation of the solution containing silver ions with γ-ray,[33−35] ultraviolet or visible light,[36−38] and microwave[39−41] and ultrasound irradiation.[23,42−46] The third route involves heating the solution of silver salt without commonly used reductants[47] or prolonged reflux silver solution in the presence of a weak reducing agent, such as glucose,[25,48] sodium citrate,[22,49] dimethylformamide,[50−52] potassium bitartrate,[53] ascorbic acid,[54] and alcohols or polyols.[12,55−57]

A variety of stabilizers or coating agents have been used in the silver preparation mentioned above to achieve the best control of size, size distribution, shape, stability, and solubility of silver nanoparticles. Thiol derivatives[27,30,39] are the most common coating agents employed to stabilize silver colloids, even though aniline,[49] long-chain amines,[8,9,58] surfactants,[10,32] starch,[48] and carboxylic compounds[9,29,31,59] have also been used. Polymers such as poly(vinyl pyrrolidone),[12,36,46,56,57] fourth-generation poly(amido amine),[60] polyacrylate,[26] polyacrylonitrile,[47] and polyacrylamide,[34,35] are also important protective agents, which can effectively control shape, size, and stability of silver nanoparticles. For example, with the refluxing method, poly(vinyl pyrrolidone) can direct the growth of silver into nanowires[12,57] and nanocubes.[56]

Furthermore, hybrid systems consisting of metal nanoparticles and organic polymers can exhibit novel combinations of particles and polymer properties. Dickson and co-worker have reported that photostable water-soluble silver nanodots created in dendrimers are quite stable and highly fluorescent.[61] Polymer-initiated photogeneration of silver nanoparticles in SPEEK/PVA (SPEEK = sulfonated poly(ether-ether) keton, PVA = poly(vinyl alcohol)) was anticipated to allow direct metal photopatterning.[62]

Here we report a one-pot reproducible route for the large-scale preparation of polyacrylamide-stabilized colloidal silver nanoparticles with bimodal size distribution. The syntheses are so simple that only three reagents of silver nitrate, monomer acrylamide, and water are needed. Neither the commonly used reductant nor initiator was needed. The obtained silver colloids are stable and easy for purification with dialysis or centrifugation to remove nitrate ions and unreacted reagents. In addition, UV−vis spectrometry, previously used to monitor the growth of silver nanowires,[57,63] is also exploited to intensively study the presence and removing of silver oxide layers covering the surface of silver nanoparticles.

II. Experimental Section

Materials. Acrylamide (AM) and silver nitrate ($AgNO_3$) were supplied by Shanghai Chemical Reagent Co. Deionized water was used throughout this work. Other reagents were of analytical grade or better and used without further purification.

Preparation. In a typical run, 1.0 g of silver nitrate and 3.5 g of acrylamide(AM) were dissolved in 50 mL of water by

* Corresponding author. Tel: +86-21-55664181. Fax: +86-21-55664192. E-mail: chenmeng@fudan.edu.cn.
† Fudan University.
‡ Lanzhou Institute of Chemical Physics, Chinese Academy of Science.
§ Institute of Physics, Chinese Academy of Science.

10.1021/jp061134n CCC: $33.50
Published on Web 05/17/2006

magnetic stirring. The resulting solution was transferred into an autoclave up to 85% of the total volume. The autoclave was maintained at a fixed temperature for 6 h and then left to air cool to room temperature. The deep-brown solution was obtained after the reaction was complete.

The Ag colloids could be purified by dialysis to remove the byproducts and polymer with smaller molecular weight and then concentrated by rotary evaporation. After being dried in a vacuum at 60 °C overnight, the composite Ag/PAM (polyacrylamide) powder could be obtained and dispersed in water again. The product could also be purified with the centrifugation−dispersion process. In this process, after the Ag/PAM colloids were cooled to room temperature, a large amount of methanol was poured into the colloid, which was centrifuged at 2000 rpm for 5 min. The resulting pellet was dissolved in water by gentle bath sonication followed by the addition of methanol, and then centrifuged again. The dispersion−centrifugation process was repeated three times to wash off the remaining residues. The final pellet was dried in a vacuum.

Instrumentation. The Fourier transform infrared (FTIR) spectra were collected on an IRPRESTIGE-21 Fourier transform infrared spectrophotometer in the wavenumber range of 400−4000 cm^{-1} at a resolution of 4 cm^{-1}. The samples were prepared in the form of pellets together with KBr. The X-ray photoelectron spectroscopy (XPS) was performed on a VGESCALAB MKII X-ray photoelectron spectrometer, using nonmonochromatized Mg−Ka X-rays as the excitation source. The binding energies obtained in the XPS analysis were corrected by referencing the C 1s peak to 284.80 eV.

The X-ray powder diffraction (XRD) pattern was recorded using a Japan Rigaku D/max γ_B-ray diffractometry in transition mode and Cu Kα radiation (λ = 1.54056 Å). Samples for measurement were prepared by dropping 5 mL of silver colloids on quartz plates and allowing them to dry at room temperature. Transmission electron microscope (TEM) images were obtained using a Hitachi H-600 electron microscope operated at 75 kV with samples deposited onto a 230-mesh copper grid covered with Formvar. Particle size analysis was carried out by manually digitizing the TEM image with Image Tool, from which the average size and standard deviation of Ag nanoparticles were generated.

The UV−vis absorption spectra were taken at room temperature on a UV-3150 spectrophotometer (Shimadzu, Japan) with a variable wavelength between 250 and 700 nm using a glass cuvette with 1-cm optical path. The thermogravimetric analysis (TGA) was performed using a Shimazu TGA-50 thermobalance (Torrance, CA) on the samples, which were dried under vacuum at 100 °C for 4 h.

III. Results and Discussion

Mechanism of the Formation of Ag/PAM Colloids. In a typical synthesis, the color of the solution changed from colorless to deep brown after the reaction of the starting mixture including 1 g of $AgNO_3$ and 3.5 g of AM heated at 150 °C. The change of color is an indication of the formation of silver nanoparticles, and the final color of the solution varies slightly with the amount of the starting materials. No peak around 300 nm, which is a characteristic of silver ions, was found in the UV−vis spectrum of the obtained silver colloid, which indicates that all of the silver ions were completely reduced.

In the present study, only three chemicals of silver nitrate, acrylamide, and water solvent are required. Neither a commonly used reducing agent for the reduction of silver ions nor an initiator for the polymerization of monomer AM was employed. The solution containing only silver nitrate in water was heated to above 150 °C, which is much lower than the decomposition temperature of silver nitrate (440 °C), and no silver particles were found. Meanwhile, heating the solution of neat acrylamide in water at 100 °C could not initiate the polymerization reaction of monomer but the spontaneous polymerization of acrylamide could take place at 120 °C or above and a certain pressure.

Colorless floccular precipitates formed when 1 g of commercial polyacrylamide was added into 50 mL of aqueous solution including 0.2 g of silver nitrate at room temperature, which indicated the coordination of silver ions with NH_2 groups in polyacrylamide, and silver ions served as weak cross-linkers to attach polymer chains. Fast formation of silver nanoparticles occurred upon exposing the above mixture to ambient (indoor) light for more than 5 min. No such process happened with the solution of acrylamide and silver nitrate in water, even when light irradiated for several days. These observations highlighted the significant role that the polymer plays in the photoreactions and also in the present preparation.

On the basis of the results of a large series of experiments and the reports on the mechanism for the reduction of silver ions, we have found that there are two possible mechanisms for the formation of silver colloids with the present technique. One involves the electron transfer from the water or acrylamide molecules to silver ions at a certain temperature, similar to that for the photolysis of silver ions in aqueous solution.[64] This mechanism can be proven by the formation of large black Ag particles visible by the naked eye when the aqueous solution of silver nitrate and acrylamide was heated to above 100 °C for 4 h, in which no obvious polyacrylamide was found. The other one is related to the reduction of silver ions by the organic radicals[33] produced in the thermal polymerization of acrylamide, which is possibly initiated by the thermal homolysis of impurities (including peroxides or hydroperoxides formed due to O_2) present in the monomer.[65]

The presence of the above two kinds of mechanisms could also be further supported by the formation of PAM-stabilized silver nanoparticles with bimodal size distribution. A small amount of silver nanoparticles formed with the first kind of mechanism in the presence of acrylamide when the temperature was less than 150 °C and grew into larger ones when the reaction proceeded. Smaller silver nanoparticles formed at the same time with the polymerization of acrylamide. As we know, thermal polymerization of olefin at relatively high temperature is a free-radical chain polymerization with a fast reaction rate. A large number of organic radicals thus formed could reduce silver ions and produce silver nanoparticles in a very short time.[33] Furthermore, reduction of silver ions and thermal polymerization of AM occurred almost simultaneously and resulted in well-dispersed Ag nanoparticles protected by polyacrylamide.

Characterization of Structure and Composition of Ag/PAM Nanocomposites. Examination of the FTIR spectra (shown in Figure 1) confirmed that the product contained the polymer of acrylamide and excluded the presence of monomer AM. The polymerization of monomer acrylamide can be ascertained by the similarity of the absorption profiles of commercial PAM (Figure 1b), neat PAM (Figure 1c) synthesized in the absence of $AgNO_3$, PAM-stabilized Ag nanoparticles (Figure 1d), and the difference from that of monomer AM (Figure 1a). For the spectrum of the PAM-stabilized Ag nanoparticles, the N−H stretching vibrations were observed at 3414 and 3188 cm^{-1}. The strong absorption at 1659 cm^{-1} can be attributed to the C═O stretching in the $-CONH_2$ group, and the shoulder around 1610 cm^{-1} to the NH_2 bending, which also

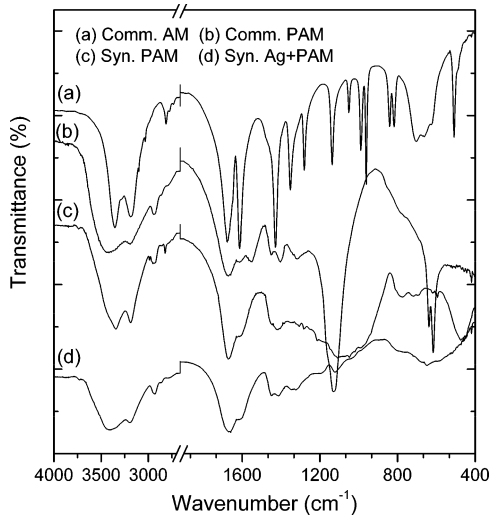

Figure 1. FTIR spectra of (a) the commercial acrylamide, (b) the commercial polyacrylamide, (c) the as-synthesized polyacrylamide, and (d) the as-synthesized Ag/polyacrylamide composites.

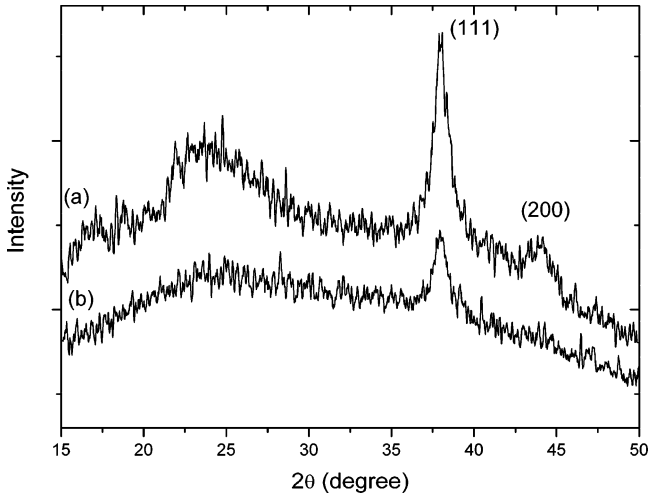

Figure 2. XRD pattern of the samples prepared from the aqueous solution containing (a) 3.5 g of polyacrylamide and 1.0 g of $AgNO_3$ and (b) 3.5 g of polyacrylamide and 0.3 g of $AgNO_3$.

indicates that PAM is stable under the reaction conditions. The frequency of the C═O stretching in Ag/PAM nanocomposites is shifted to 1659 cm^{-1} from 1670 cm^{-1} of that in commercial PAM or neat PAM, which implies the presence of coordination of Ag atoms with the oxygen atoms in carbonyl group.[34] But no obvious shift of the absorption peak of N−H at 1610 cm^{-1} was observed.

The XRD pattern of as-prepared particles (Figure 2) shows broad peaks around 38° and 44° corresponding to (111), (200) of the cubic silver structures within experimental error. Only one or two peaks were observed because of the low concentration of silver nanoparticles in the product. With increasing $AgNO_3$ content in the starting solution, the characteristic peaks of the resultant product became stronger. The broad peak at 2θ less than 40° is attributed to the noncrystalline polymer PAM, which also causes the higher uneven baseline. The XRD analysis further proved that Ag/PAM nanocomposites had been achieved with the simple route.

To obtain some detailed knowledge about the chemical composition of the polyacrylamide-stabilized silver nanoparticles, X-ray photoelectron spectroscopic (XPS) studies have been carried out. Figure 3 shows the XPS spectra of the stabilized silver nanoparticles with all of the binding energies referenced to C 1s (284.8 eV). The survey spectrum (shown in Figure 3a) reveals the existence of C and O, which are, from reference, polymer stabilizer and absorbed gaseous molecules, respectively. Higher resolution spectra were also taken of the Ag 3d region. In Figure 3b, the binding energies of Ag $3d_{5/2}$ and Ag $3d_{3/2}$ of the passivated silver nanoparticles are 368.5 and 374.5 eV. No impurity peaks of pure Ag^+ and Ag_2O particles were observed.

Dried samples in an N_2 atmosphere have been subjected to thermogravimetric (TG) analysis in the 30−600 °C range (shown in Figure 4). Three samples were prepared from the starting solutions with 3.5 g of acrylamide and 0 (sample a), 0.1 (sample b), and 1.0 g (sample c) of $AgNO_3$, respectively, but undergoing the same heating temperature and time. The profiles of all of the samples showed that there were three stages of mass loss for the thermal degradation of polyacrylamide, which is in agreement with that reported.[66] The first one involved a slight weight loss with temperature below 220 °C for the synthesized pure PAM, which is probably due to absorbed water from the environment and other volatile impurities.[67] For the composite samples with Ag nanoparticles, a weight loss of around 15% could be observed in this region. Vilcu et al. observed an 11% weight loss up to 200 °C, which they attributed to the release of both surface and matrix-bound water from the polymer.[68] In the present study, it is most likely that the presence of Ag nanoparticles enhanced the water absorbance of PAM. The second one appeared in the range of 220−340 °C with the decomposition of pendant amide groups

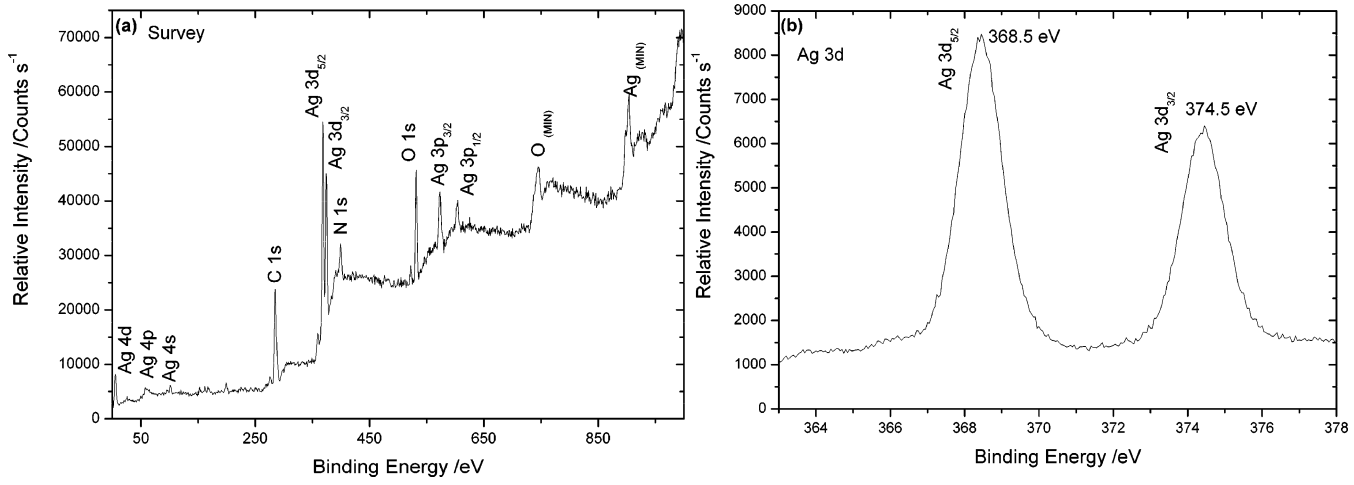

Figure 3. XPS spectra of the polyacrylamide passivated silver nanoparticles: (a) the survey spectrum and (b) the close-up spectrum of Ag 3d.

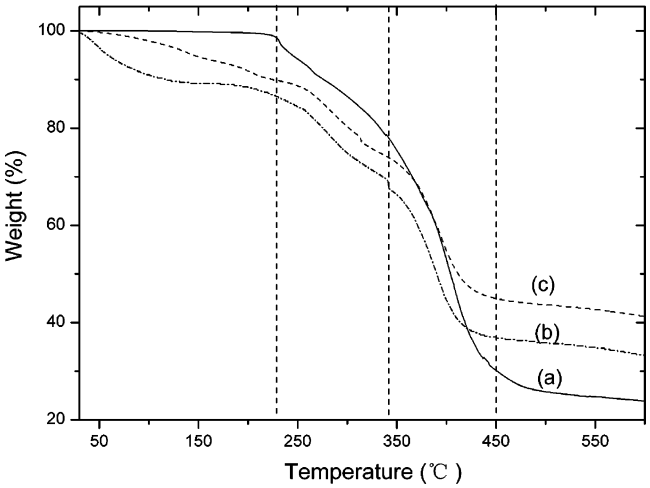

Figure 4. TG curves for the samples heated to 600 °C. The samples are prepared from the starting solutions including 3.5 g of acrylamide and (a) 0, (b) 0.1, and (c) 1.0 g of $AgNO_3$, respectively.

and the intactness of polymer main chains.[69] The observed values of weight loss are around 20%, 17%, and 17% for samples a, b, and c, respectively. The third one (340−450 °C) with 48%, 32%, and 30% of weight loss for the different samples, respectively, could be ascribed to the breakdown of the polymer backbones.[69] It is reasonable that the remaining weight increased with increasing the $AgNO_3$ content in the starting solutions.

Study of Ag Colloids with UV−Vis Spectra, Light Scattering Simulation, and TEM. UV−vis absorption measurements can provide a deeper insight into the optical properties of the formed particles, confirming that we are really dealing with nanosized Ag particles and give some information about the size, size distribution, and surface properties of Ag nanoparticles. Figure 5a shows the UV−vis plasmon absorption of the product obtained from the solution containing 1.75 g of AM and 0.6 g of $AgNO_3$ in water. Broad surface plasmon resonance (SPR) bands from 350 to 450 nm can be seen in the spectrum along with a distinct maximum at ca. 450 nm; there are two shoulders at 420 and 350 nm or so. In most cases, the presence of two or more SPR bands indicated the formation of anisotropic silver nanoparticles. On the basis of Mie's theory,[70] spherical silver nanoparticles could give a single symmetric absorption band around 410 nm, whereas anisotropic nanoparticles should exhibit two or more bands. A number of experiments have also proven this theory and given similar results.[16,19,20,23,57,63,71]

In the present study, we supposed that the appearance of a broad band consisting of three peaks implied that a thin layer of silver oxide (Ag_2O) formed on the surface of silver nanoparticles, and the colloids were the mixture of silver nanoparticles with and without silver oxide layers. The shoulder peak around 420 nm was indicative of the presence of silver

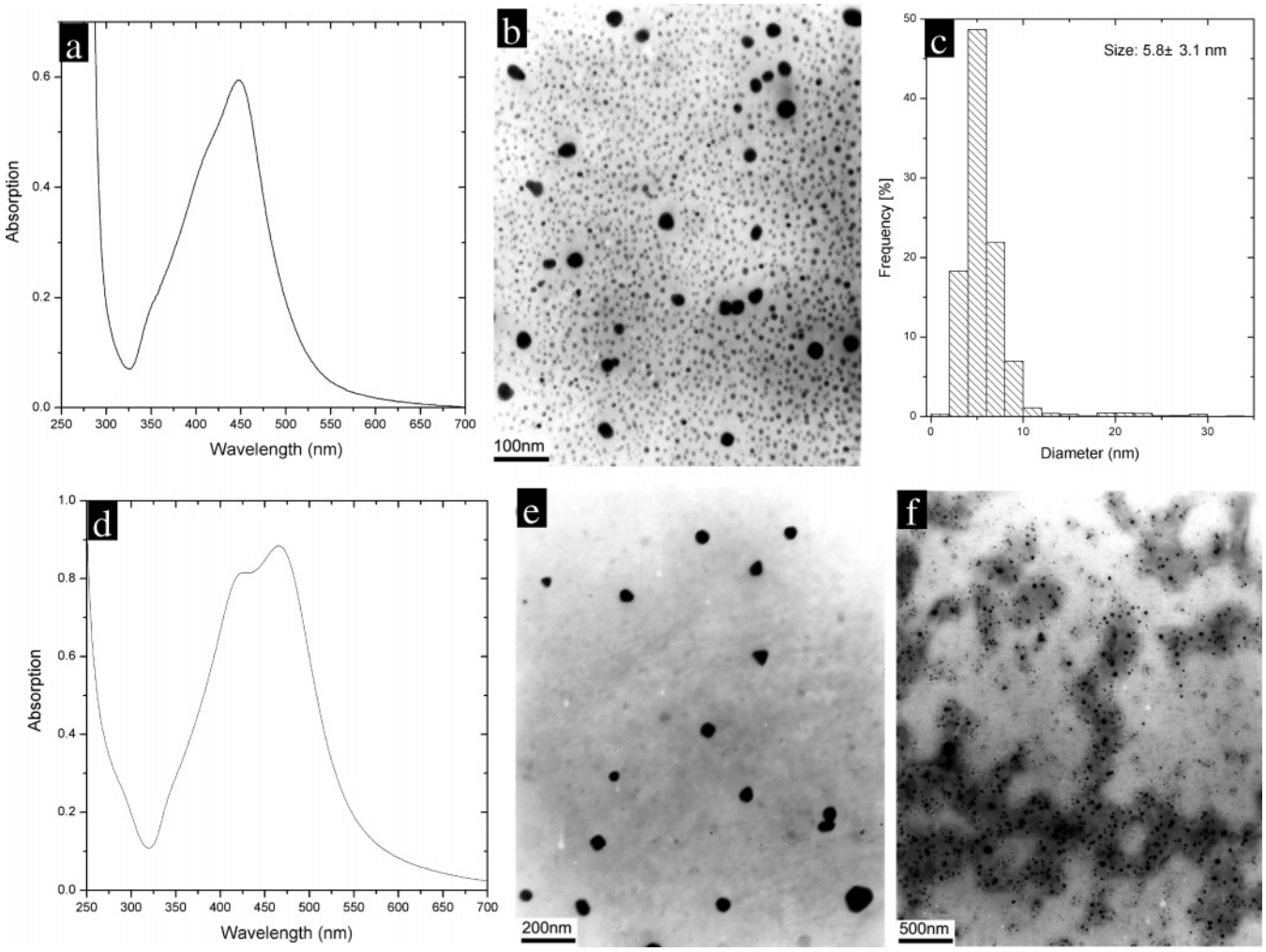

Figure 5. (a) UV−vis absorption spectrum, (b) TEM image, and (c) histogram of size distribution of the sample prepared from the solution containing 1.75 g of AM and 0.6 g of $AgNO_3$ in water. (d) UV−vis absorption spectrum and (e, f) TEM images of the sample from the solution containing 3.5 g of AM and 1.0 g of $AgNO_3$ in water.

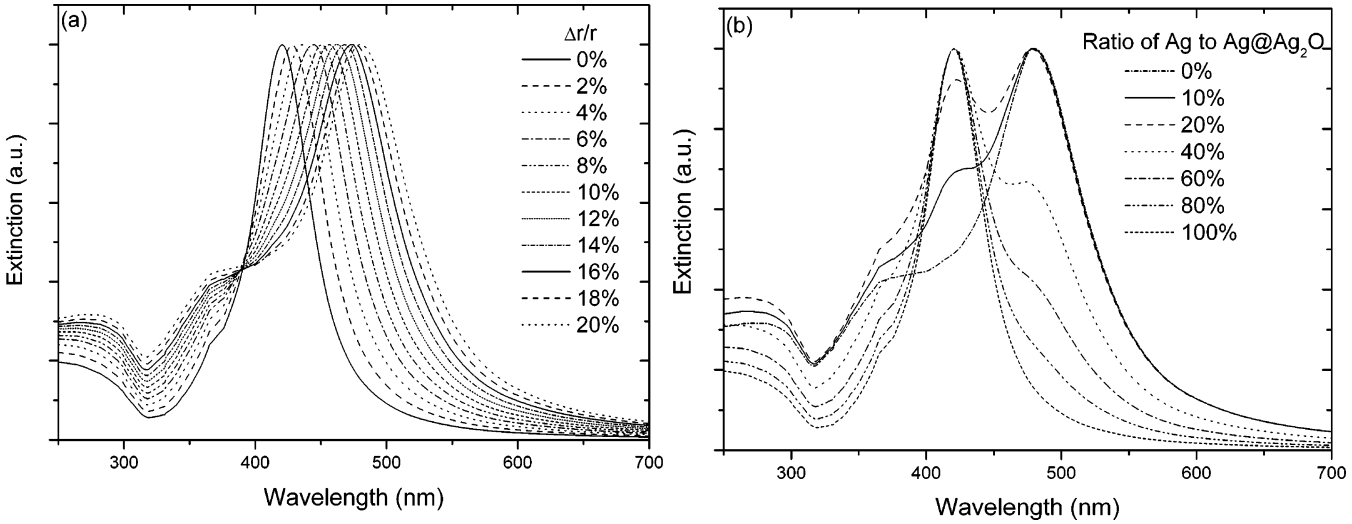

Figure 6. (a) Simulated absorption curves (after normalization) of 25 nm silver nanoparticles with different oxidation percentages. Here, Δr stands for the thickness of Ag_2O and r is the radius of Ag nanoparticles before oxidation and equals 25 nm. (b) The simulated absorption curves (after normalization) of the mixture including Ag nanoparticles ($r = 25$ nm) and Ag@Ag_2O particles ($\Delta r/r = 20\%$) with different ratios.

nanoparticles without Ag_2O layers, and the absorption band at ca. 450 nm suggested the existence of Ag/Ag_2O core−shell structures. The intensity of the peak implied the amount of the corresponding structure in the sample, and the thickness of Ag_2O layers on the Ag surface could be inferred from the position of the absorption band at ca. 450−470 nm.

The above conclusions could be further supported by the following studies. Xia's group[72] has intensively investigated the red-shift of surface plasmon peaks of silver nanoparticles with experimental and simulation studies and concluded that the oxidation of the surfaces of silver nanoparticles should be responsible for the red-shift and broadening of the surface plasmon band of silver nanoparticles. In the study, a classic electrodynamic model was also used to simulate the absorption spectra of the obtained silver colloids. We assumed that our colloidal system was an ideal monodispersed silver nanoparticle without the effect of polyacrylamide on UV−vis absorption. Figure 6 shows the simulation results, which are in good agreement with the above summary. Absorption spectra similar to the profiles of the simulated curves shown in Figure 6b were often observed in our experimental results, which confirmed that the as-obtained colloids were the mixture of Ag and Ag@Ag_2O nanoparticles with their ratio depending on the reaction conditions.

Generally speaking, our experimental results showed that extending the heating time, increasing the ratio of AM to $AgNO_3$, or increasing the heating temperature from 150 to 180 °C favored the oxidation of silver nanoparticles, which resulted in the increase of the intensity of absorption band around 450−470 nm and the decrease of that of the peak at ca. 420 nm.

In the present research work, the surface of silver nanoparticles is oxidized because of the heating reaction with relative high temperature in the presence of oxygen-contained monomer and high oxidative NO_3^-. The fact that heating reaction conditions leads to the formation of surface species Ag_2O has been reported by Sun et al.[73] In addition, Pol et al.[74] also claimed that silver oxide was found to exist on the surface of silica core−silver shell nanostructures prepared without bubbling argon gas prior to sonication. Kapoor's group recently asserted that electron transfer from silver nanoparticles to chloroform or toluene is facilitated in the presence of oxygen.[75] On the basis of the reports about surface chemistry of colloidal silver in aqueous solution,[76,77] the silver atoms on the surface of

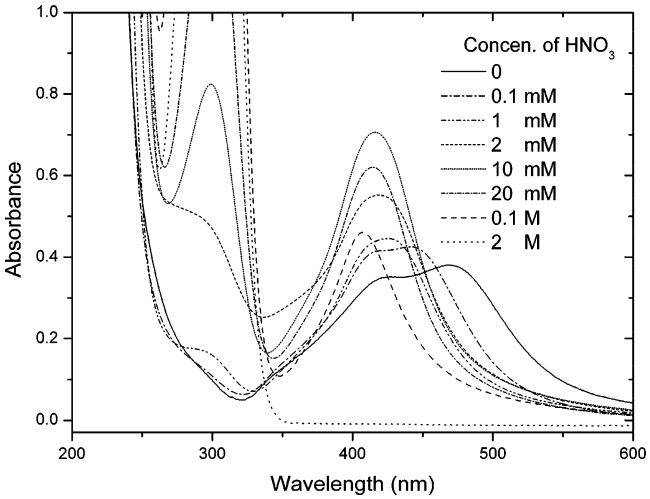

Figure 7. UV−vis absorption spectra of the colloidal Ag solution prepared by dropping 10 μL of AM-stabilized silver colloids into 6 mL of HNO_3 solutions with concentrations of 0, 0.1 mM, 1 mM, 2 mM, 10 mM, 20 mM, 0.1 M, and 2M.

nanoparticles are coordinatively unsaturated, and polyacrylamide serving as a nucleophilic reagent can donate an electron pair into unoccupied orbitals that exist on the surface. Silver nanoparticles with nucleophilic molecules on the surface are very reactive toward oxygen and oxidative reagents, which lead to further complexation of surface atoms until the particle is whole or partly oxidized.

Figure 5b and c illustrates the typical TEM image and size distribution of the corresponding silver samples. Not only are nearly spherical Ag nanoparticles about 5.0 nm observed but a few large individual Ag nanoparticles with sizes between 10 and 30 nm are also shown in the image. Reproducible experiments and TEM characterization under different conditions always gave the nanoparticles with bimodal size distribution. The TEM images (shown in Figure 5e and f) of the samples prepared with the starting solution containing 3.5 g of AM and 1.0 g of $AgNO_3$ are obtained from two different parts on the copper grid. It is obvious that the average size of the as-obtained Ag nanoparticles increased with increasing the amount of $AgNO_3$ from 0.6 to 1 g. In Figure 5f, the image contrast between gray polymers and black Ag nanoparticles can be clearly observed, which indicates the coating and stabilization of PAM

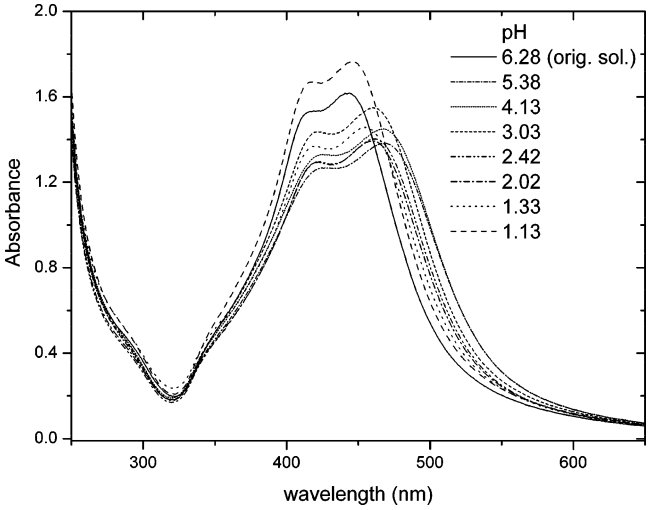

Figure 8. UV−vis absorption spectra of the colloidal Ag solution with the pH value adjusted by dilute HNO_3 solutions.

on Ag nanoparticles. In addition, there are still a few large Ag nanoparticles with an average size of 50 nm besides a large amount of small particles in the size range of 17.4 ± 13.9 nm (shown in Figure 5e). The two kinds of different reaction mechanisms might be responsible for the formation of silver nanoparticles with bimodal size distribution as stated before.

Evolution of UV−Vis Spectra of Ag Colloids after Addition of Acids and Salts. UV−vis spectroscopic monitoring of the dissolution of the silver nanoparticles in HNO_3 solutions of different concentration further confirmed the presence of Ag_2O layers. Figure 7 is the UV−vis spectra of the solution by dropping 10 μL of AM-stabilized silver colloids into 6 mL of HNO_3 solutions with different concentrations. As the concentration of HNO_3 increased from 0 to 2 M, The distinct broad peak, which is located at ca. 450 nm and belonging to Ag@Ag_2O core−shell nanoparticles, vanished gradually and merged into the shoulder band that belongs only to Ag nanoparticles, and formed a relatively symmetric peak whose location is eventually blue-shifted to 413 nm. At the same time, another peak at 300 nm appeared and its intensity increased with the HNO_3 concentration increasing, which inferred the gradual dissolution of silver oxide layer and some of neat silver nanoparticles and the formation of silver ions.

The intensity, on the other hand, of the absorption peak at around 413 nm increased as the HNO_3 concentration changed from 0.1 mM to 10 mM, and then decreased with the HNO_3 concentration increased to 2 M from 10 mM; meanwhile, a significant increase in intensity of the peak at 300 nm was also observed. The intensity variation of both peaks depending on the HNO_3 concentration reveals the following conclusions: (1) The removing of silver oxide layers from the surfaces of silver nanoparticles resulted in the increase of the intensity of the SPR peak for silver nanoparticles. (2) Dissolution of Ag nanoparticles led to the decrease of the intensity of the SPR peak for Ag nanoparticles and the increase of the intensity of silver ions. Thus, it is most likely to control the thickness of Ag_2O layers on the surface of Ag nanoparticles by adjusting pH value of the colloids with dilute HNO_3 solution. However, we found that the absorption peak around 450 nm was red-shifted to around 470 nm when the pH value of the AM-stabilized Ag colloids was changed from 6.28 to 5.38 or 4.13 and then blue-shifted to 450 nm when the pH value was decreased from 4.13 to 1.13 (shown in Figure 8). The variation of the position of the absorption peak indicated that the thickness of Ag_2O layers was increased with the addition of a small amount of very dilute HNO_3 solution (shown in eq 1), and then part of Ag_2O layers was removed when more HNO_3 was used (shown in eq 2).

$$2Ag + 2HNO_3 \rightarrow Ag_2O\downarrow + 2NO_2\uparrow + H_2O \qquad (1)$$

$$Ag_2O + 2HNO_3 \rightarrow 2AgNO_3 + H_2O \qquad (2)$$

To fully prove the existence of silver nanoparticles covered with Ag_2O layers, we replaced HNO_3 with acetic acid (HAc) and NaCl solution. AM-stabilized silver colloids (50 μL) were added to 6 mL of 5 M NaCl solutions. Figure 9a is the UV−vis spectra of the colloids before and after the addition. The broad SPR bands between 350 and 550 nm disappeared, and a relatively symmetric peak at around 412 nm could be observed, indicating that the Ag_2O layers were completely removed and the AM-stabilized pure silver nanoparticles were present. In addition, a small shoulder at ca. 280 nm was also seen owing to the formation of AgCl particles.[78,79] The mechanism for the formation of AgCl might involve the following chemical reaction:

$$Ag_2O + H_2O + 2NaCl \rightarrow 2AgCl\downarrow + 2NaOH \qquad (3)$$

Similar results have also been achieved when adding 60 μL of AM-stabilized silver colloids into 6 mL of HAc solutions

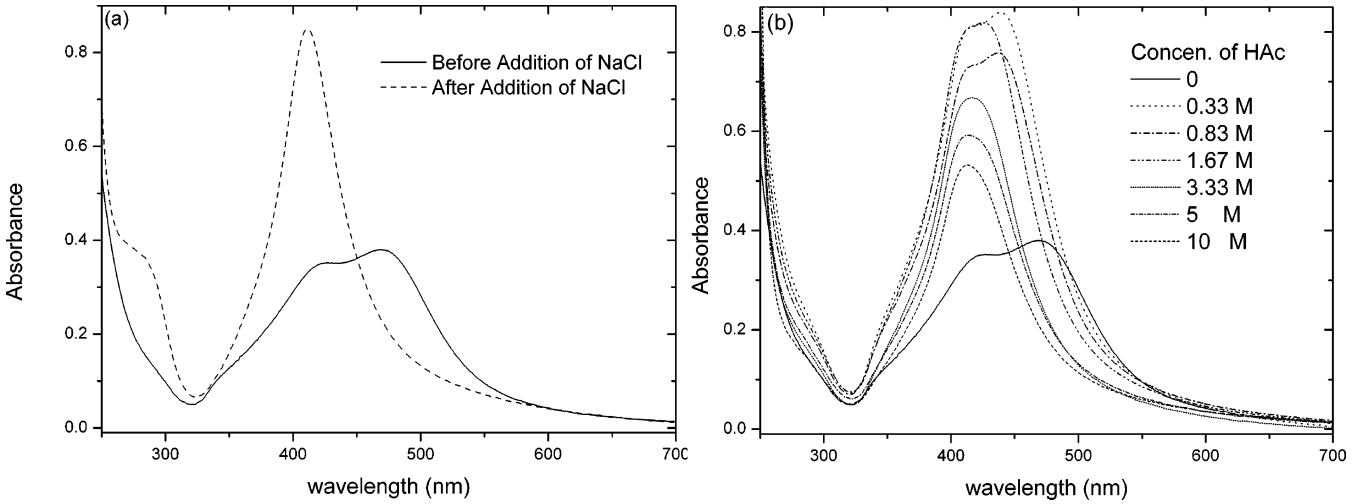

Figure 9. UV−vis absorption spectra of the colloidal Ag solution with the addition of (a) NaCl solution and (b) HAc solutions of different concentration.

with different concentrations (shown in Figure 9b). The reason for the appearance of a relatively symmetric peak positioned at ca. 410 nm is that the ultrathin Ag_2O layers were dissolved by HAc and PAM-stabilized pure Ag nanoparticles appeared gradually.

IV. Conclusions

We have prepared well-dispersed polyacrylamide-stabilized silver nanoparticles with bimodal size distribution in the absence of any commonly used reducing agent for reduction and any initiator for polymerization. A possible mechanism for the formation of silver nanoparticles with bimodal size distribution was proposed. In addition, light scattering simulation and UV−vis absorption studies confirmed that the obtained colloids were the mixture of Ag and Ag_2O nanoparticles. The presence of silver oxide layers on the nanoparticle surface resulted in the broadening of the surface plasmon band of silver nanoparticles. Ag_2O layers could be added or removed from Ag nanoparticle surfaces by the addition of HNO_3, HAc, or NaCl solution to the as-obtained silver colloids.

Acknowledgment. This research work was financially supported by the Scientific Research Foundation for the Returned Overseas Chinese Scholars, Ministry of Education, P R China, and the National Natural Science Foundation of China (no. 20473024). Z.Y.L. was supported by the National Natural Science Foundation of China (no. 10525419).

References and Notes

(1) Evanoff, D. D.; Chumanov, G. *Chemphyschem* **2005**, *6*, 1221−1231.
(2) Evanoff, D. D.; Chumanov, G. *J. Phys. Chem. B* **2004**, *108*, 13957−13962.
(3) El-Sayed, M. A. *Acc. Chem. Res.* **2001**, *34*, 257−264.
(4) Link, S.; El-Sayed, M. A. *J. Phys. Chem. B* **1999**, *103*, 8410−8426.
(5) Jana, N. R.; Sau, T. K.; Pal, T. *J. Phys. Chem. B* **1999**, *103*, 115−121.
(6) Morones, J. R.; Elechiguerra, J. L.; Camacho, A.; Holt, K.; Kouri, J. B.; Ramirez, J. T.; Yacaman, M. J. *Nanotechnology* **2005**, *16*, 2346−2353.
(7) Jeong, S. H.; Hwang, Y. H.; Yi, S. C. *J. Mater. Sci.* **2005**, *40*, 5413−5418.
(8) Hiramatsu, H.; Osterloh, F. E. *Chem. Mater.* **2004**, *16*, 2509−2511.
(9) Jana, N. R.; Peng, X. G. *J. Am. Chem. Soc.* **2003**, *125*, 14280−14281.
(10) Taleb, A.; Petit, C.; Pileni, M. P. *Chem. Mater.* **1997**, *9*, 950−959.
(11) Evanoff, D. D.; Chumanov, G. *J. Phys. Chem. B* **2004**, *108*, 13948−13956.
(12) Sun, Y. G.; Xia, Y. N. *Adv. Mater.* **2002**, *14*, 833−837.
(13) Xiong, Y. J.; Xie, Y.; Wu, C. Z.; Yang, J.; Li, Z. Q.; Xu, F. *Adv. Mater.* **2003**, *15*, 405-+.
(14) Choi, J.; Sauer, G.; Nielsch, K.; Wehrspohn, R. B.; Gosele, U. *Chem. Mater.* **2003**, *15*, 776−779.
(15) Caswell, K. K.; Bender, C. M.; Murphy, C. J. *Nano Lett.* **2003**, *3*, 667−669.
(16) Sun, Y. G.; Mayers, B.; Herricks, T.; Xia, Y. N. *Nano Lett.* **2003**, *3*, 955−960.
(17) Germain, V.; Brioude, A.; Ingert, D.; Pileni, M. P. *J. Chem. Phys.* **2005**, *122*.
(18) Chen, S. H.; Fan, Z. Y.; Carroll, D. L. *J. Phys. Chem. B* **2002**, *106*, 10777−10781.
(19) Maillard, M.; Giorgio, S.; Pileni, M. P. *J. Phys. Chem. B* **2003**, *107*, 2466−2470.
(20) Jin, R. C.; Cao, Y. W.; Mirkin, C. A.; Kelly, K. L.; Schatz, G. C.; Zheng, J. G. *Science* **2001**, *294*, 1901−1903.
(21) Sarkar, A.; Kapoor, S.; Mukherjee, T. *J. Colloid Interface Sci.* **2005**, *287*, 496−500.
(22) Sun, Y. G.; Mayers, B.; Xia, Y. N. *Nano Lett.* **2003**, *3*, 675−679.
(23) Jiang, L. P.; Xu, S.; Zhu, J. M.; Zhang, J. R.; Zhu, J. J.; Chen, H. Y. *Inorg. Chem.* **2004**, *43*, 5877−5883.
(24) Im, S. H.; Lee, Y. T.; Wiley, B.; Xia, Y. N. *Angew. Chem., Int. Ed.* **2005**, *44*, 2154−2157.
(25) Yu, D. B.; Yam, V. W. W. *J. Am. Chem. Soc.* **2004**, *126*, 13200−13201.
(26) Zhang, Z. Q.; Patel, R. C.; Kothari, R.; Johnson, C. P.; Friberg, S. E.; Aikens, P. A. *J. Phys. Chem. B* **2000**, *104*, 1176−1182.
(27) Shon, Y. S.; Cutler, E. *Langmuir* **2004**, *20*, 6626−6630.
(28) Bagwe, R. P.; Khilar, K. C. *Langmuir* **2000**, *16*, 905−910.
(29) Wang, W.; Efrima, S.; Regev, O. *Langmuir* **1998**, *14*, 602−610.
(30) He, S. T.; Yao, J. N.; Xie, S. S.; Gao, H. J.; Pang, S. J. *J. Phys. D: Appl. Phys.* **2001**, *34*, 3425−3429.
(31) Wang, W.; Chen, X.; Efrima, S. *J. Phys. Chem. B* **1999**, *103*, 7238−7246.
(32) LizMarzan, L. M.; LadoTourino, I. *Langmuir* **1996**, *12*, 3585−3589.
(33) Henglein, A.; Giersig, M. *J. Phys. Chem. B* **1999**, *103*, 9533−9539.
(34) Yang, Q.; Wang, F.; Tang, K. B.; Wang, C. R.; Chen, Z. W.; Qian, Y. T. *Mater. Chem. Phys.* **2002**, *78*, 495−500.
(35) Zhu, Y. J.; Qian, Y. T.; Li, X. J.; Zhang, M. W. *Chem. Commun.* **1997**, 1081−1082.
(36) Huang, H. H.; Ni, X. P.; Loy, G. L.; Chew, C. H.; Tan, K. L.; Loh, F. C.; Deng, J. F.; Xu, G. Q. *Langmuir* **1996**, *12*, 909−912.
(37) Yanagihara, N.; Tanaka, Y.; Okamoto, H. *Chem. Lett.* **2001**, 796−797.
(38) Callegari, A.; Tonti, D.; Chergui, M. *Nano Lett.* **2003**, *3*, 1565−1568.
(39) Gao, F.; Lu, Q. Y.; Komarneni, S. *Chem. Mater.* **2005**, *17*, 856−860.
(40) Zhu, Y. J.; Hu, X. L. *Mater. Lett.* **2004**, *58*, 1517−1519.
(41) Tsuji, M. L.; Nishizawa, Y.; Hashimoto, M.; Tsuji, T. *Chem. Lett.* **2004**, *33*, 370−371.
(42) Xiong, Y. J.; Xie, Y.; Du, G. O.; Liu, X. M.; Tian, X. B. *Chem. Lett.* **2002**, 98−99.
(43) Zhang, J. L.; Han, B. X.; Liu, M. H.; Liu, D. X.; Dong, Z. X.; Liu, J.; Li, D.; Wang, J.; Dong, B. Z.; Zhao, H.; Rong, L. X. *J. Phys. Chem. B* **2003**, *107*, 3679−3683.
(44) Salkar, R. A.; Jeevanandam, P.; Aruna, S. T.; Koltypin, Y.; Gedanken, A. *J. Mater. Chem.* **1999**, *9*, 1333−1335.
(45) Malandrino, G.; Finocchiaro, S. T.; Fragala, I. L. *J. Mater. Chem.* **2004**, *14*, 2726−2728.
(46) Carotenuto, G.; Pepe, G. P.; Nicolais, L. *Eur. Phys. J. B* **2000**, *16*, 11−17.
(47) Zhang, Z. P.; Han, M. Y. *J. Mater. Chem.* **2003**, *13*, 641−643.
(48) Raveendran, P.; Fu, J.; Wallen, S. L. *J. Am. Chem. Soc.* **2003**, *125*, 13940−13941.
(49) Tan, Y. W.; Li, Y. F.; Zhu, D. B. *J. Colloid. Interface Sci.* **2003**, *258*, 244−251.
(50) Pastoriza-Santos, I.; Liz-Marzan, L. M. *Langmuir* **1999**, *15*, 948−951.
(51) Pastoriza-Santos, I.; Liz-Marzan, L. M. *Pure Appl. Chem.* **2000**, *72*, 83−90.
(52) Giersig, M.; Pastoriza-Santos, I.; Liz-Marzan, L. M. *J. Mater. Chem.* **2004**, *14*, 607−610.
(53) Tan, Y. W.; Dai, X. H.; Li, Y. F.; Zhu, D. B. *J. Mater. Chem.* **2003**, *13*, 1069−1075.
(54) Lee, G. J.; Shin, S. I.; Kim, Y. C.; Oh, S. G. *Mater. Chem. Phys.* **2004**, *84*, 197−204.
(55) Silvert, P. Y.; HerreraUrbina, R.; Duvauchelle, N.; Vijayakrishnan, V.; Elhsissen, K. T. *J. Mater. Chem.* **1996**, *6*, 573−577.
(56) Sun, Y. G.; Xia, Y. N. *Science* **2002**, *298*, 2176−2179.
(57) Sun, Y. G.; Yin, Y. D.; Mayers, B. T.; Herricks, T.; Xia, Y. N. *Chem. Mater.* **2002**, *14*, 4736−4745.
(58) Green, M.; Allsop, N.; Wakefield, G.; Dobson, P. J.; Hutchison, J. L. *J. Mater. Chem.* **2002**, *12*, 2671−2674.
(59) Lin, X. Z.; Teng, X. W.; Yang, H. *Langmuir* **2003**, *19*, 10081−10085.
(60) Manna, A.; Imae, T.; Aoi, K.; Okada, M.; Yogo, T. *Chem. Mater.* **2001**, *13*, 1674−1681.
(61) Zheng, J.; Dickson, R. M. *J. Am. Chem. Soc.* **2002**, *124*, 13982−13983.
(62) Korchev, A. S.; Bozack, M. J.; Slaten, B. L.; Mills, G. *J. Am. Chem. Soc.* **2004**, *126*, 10−11.
(63) Hu, J. Q.; Chen, Q.; Xie, Z. X.; Han, G. B.; Wang, R. H.; Ren, B.; Zhang, Y.; Yang, Z. L.; Tan, Z. Q. *Adv. Funct. Mater.* **2004**, *14*, 183−189.
(64) Hada, H.; Yonezawa, Y.; Yoshida, A.; Kurakake, A. *J. Phys. Chem.* **1976**, *80*, 2728−2731.
(65) Odian, G. *Principles of Polymerization*, fourth ed.; John Wiley & Sons: New Jersey, 2004.
(66) Caulfield, M. J.; Qiao, G. G.; Solomon, D. H. *Chem. Rev.* **2002**, *102*, 3067−3083.
(67) Silva, M.; Dutra, E. R.; Mano, V.; Machado, J. C. *Polym. Degrad. Stab.* **2000**, *67*, 491−495.

(68) Vilcu, R.; Irinei, F.; Ionescubujor, J.; Olteanu, M.; Demetrescu, I. *J. Therm. Anal.* **1985**, *30*, 495−502.
(69) Vandyke, J. D.; Kasperski, K. L. *J. Polym. Sci., Part A: Polym. Chem.* **1993**, *31*, 1807−1823.
(70) Mie, G. *Ann. Phys.* **1908**, *25*, 377.
(71) Sun, Y. G.; Gates, B.; Mayers, B.; Xia, Y. N. *Nano Lett.* **2002**, *2*, 165−168.
(72) Yin, Y. D.; Li, Z. Y.; Zhong, Z. Y.; Gates, B.; Xia, Y. N.; Venkateswaran, S. *J. Mater. Chem.* **2002**, *12*, 522−527.
(73) Sun, X. P.; Dong, S. J.; Wang, E. K. *Macromolecules* **2004**, *37*, 7105−7108.
(74) Pol, V. G.; Srivastava, D. N.; Palchik, O.; Palchik, V.; Slifkin, M. A.; Weiss, A. M.; Gedanken, A. *Langmuir* **2002**, *18*, 3352−3357.
(75) Sarkar, A.; Kapoor, S.; Mukherjee, T. *J. Phys. Chem. B* **2005**, *109*, 7698−7704.
(76) Mulvaney, P.; Linnert, T.; Henglein, A. *J. Phys. Chem.* **1991**, *95*, 7843−7846.
(77) Vukovic, V. V.; Nedeljkovic, J. M. *Langmuir* **1993**, *9*, 980−983.
(78) Calandra, P.; Longo, A.; Marciano, V.; Liveri, V. T. *J. Phys. Chem. B* **2003**, *107*, 6724−6729.
(79) Cheng, D. M.; Xia, H. B.; Chan, H. S. O. *Langmuir* **2004**, *20*, 9909−9912.